# Fatigue Crack Propagation Evaluated by Electric Resistance and Ultrasonics in Copper Film Bonded to Base Metal with Resin

Donghui MA

*Graduate student, Graduate School
of Natural Science and Technology,
Okayama University, Okayama, Japan*

Tashiyuki TORII, Kenichi SHIMIZU

*Graduate School of Natural Science
and Technology, Okayama University,
Okayama, Japan*

Akira MATSUBA

*Hiroshima Prefectural
Technology Research Institute,
Hiroshima, Japan*

(Received November 28, 2007)

**Abstract**: As model specimens of surface film-bonded materials, pure copper films with a thickness of 100μm were bonded to the surface of steel base with epoxy resin, where the tensile residual stress was measured by an X-ray on the surface copper film. The distribution of initial electric resistance was measured on both copper film and base specimen by a direct current potential drop technique. As a result, there was a good agreement between the measured and theoretical values. From the fatigue testing results, it was shown that the measured electric resistance increased with the fatigue crack length on the copper film, which was almost equal to the theoretical value calculated for a central slit in a plate with finite width. This was probably because the fatigue crack was opened due to the tensile residual stress on the film even under unloading condition. In addition, the internal crack length during fatigue was examined by ultrasonic testing for the film-bonded specimen. As a result, there was a difference in the fatigue crack length between the surface copper film and the inner base.

## 1.INTRODUCTION

In recent years, copper films have been widely used as wiring material in the printed wiring board because of the superior conductivity for miniaturization and lightweight of the electronic parts and machine. Especially, in order to improve heat radiation of the metal core wiring board, copper films with conductivity are bonded with insulation resin to the surface of metal base plate[1]. Since such electronic components are often subjected to cyclic deformation by heat loading and mechanical vibration, fatigue damage is caused during operation[2-4]. Generally, the change of electric resistance in connection with functional properties of the electronic parts is related with fatigue crack initiation and propagation in metalic materials. From this, it is possible that fatigue crack propagation lives will be evaluated by measuring the electric resistance on the surface copper film, even if the fatigue crack can not be observed by visual measurement during operation. In the connection with the laminated composite, it is important to discuss the fatigue crack propagation behavior from the surface film to the inner base through the bonded epoxy layer.

In this study, model specimens with pure copper films bonded to the surface of steel base with epoxy resin were prepared, as well as in the previous paper[5]. Using both specimens of the film-bonded specimen and the steel base specimen, the fatigue crack propagation was examined by the electric resistance change, and then the crack opening due to tensile residual stress on the surface copper film was discussed based on the electric resistance change. Finally, the fatigue crack propagation on surface copper film was discussed in relation to the internal crack propagation by using ultrasonic testing in the film-bonded specimen.

## 2.EXPERIMENTAL PROCEDURES

### 2.1. Specimens

Chemical compositions of medium carbon steel (S45C) used as the base and the pure copper film are shown in Table 1. Material properties of the base, film and the epoxy resin employed as an adhesive are shown in Table 2. Using these materials, specimens with the dimension shown in Fig. 1 were prepared. The steel base was annealed at 1173 K for one hour and machined, then annealed at 873 K for one hour to eliminate residual stress due to machining. The cold rolled pure copper films with the thickness of $t_f$=100 μm were shaped for a rectangle of 30×50 mm$^2$, and polished to mirror surface, finally annealed at 873 K for one hour in a vacuum furnace. Subsequently, the copper films were bonded to both sides of the base with the epoxy resin at 373 K for one hour, where teflon sheets with the thickness of 50 μm were inserted between the copper film and the base at both ends as shown in Fig. 1, thereby preventing contact completely between these materials. In addition, the measured thickness of epoxy bonding layer, $t_s$, of all the specimens was in the range from 47 to 106 μm.

Finally, a circular through hole with a diameter of 0.5 mm was drilled at the center of the specimen as a notch shown in Fig. 1 so that the fatigue crack could be initiated from the notch root. The face along thickness of the notch hole was

*E-mail: kshimizu@mech.okayama-u.ac.jp

104

polished with alumina powder and silk thread as shown in Fig. 2. This type of the specimen is referred to as the epoxy-bonded copper film. Moreover, the reference specimen of base itself was also prepared for the purpose of comparing with epoxy-bonded copper film in electric resistance change during fatigue crack propagation.

## 2.2. Fatigue testing

Fatigue testing was performed using a servo-hydraulic testing machine(Shimadzu Servopet Lab5), where all the

Table 1. Chemical compositions.

|  |  |  |  |  |  |  | mass % |
|---|---|---|---|---|---|---|---|
|  | Al | Ni | Sn | Pb | Fe | Zn | Mn |
| Cu (film) | 0.00005> | 0.00005> | 0.00005> | 0.00005> | 0.00005> | 0.00005> | 0.00004 |

|  | C | Si | Mn | P | S |
|---|---|---|---|---|---|
| S45C (base) | 0.45 | 0.18 | 0.78 | 0.012 | 0.006 |

Table 2. Material properties.

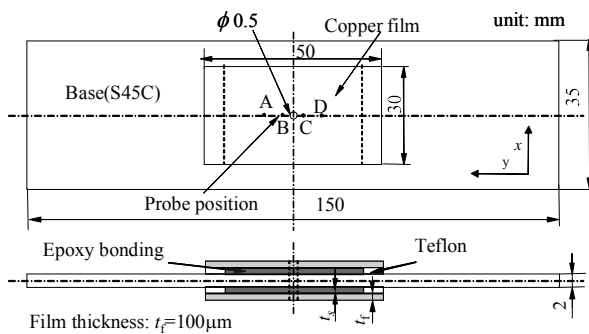|  | Young's modulus E GPa | Density $\rho$ kg/m$^3$ | Poisson's ratio $\nu$ | Linear thermal expansion coefficient $\alpha$ /K |
|---|---|---|---|---|
| Base (S45C) | 206 | $7.8 \times 10^3$ | 0.30 | $1.10 \times 10^{-5}$ |
| Cu | 123 | $8.93 \times 10^3$ | 0.34 | $1.68 \times 10^{-5}$ |
| Epoxy | 5.4 | $1.49 \times 10^3$ | 0.38 | $4.0 \times 10^{-5}$ |


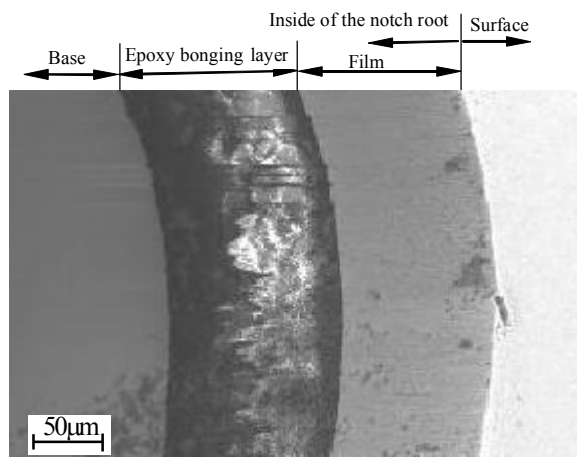
Fig. 1. Dimension of specimen.



Fig. 2. SEM micrograph observed along the thickness of the notch hole.

specimens were subjected to a push-pull cyclic loading under a constant sinusoidal wave and the testing frequency of 20 Hz. Stress amplitude of $\sigma_a$=140 MPa with stress ratio of R=−1 was loaded to the base plate. In addition, the length of fatigue crack on the surface was measured by an optical microscope.
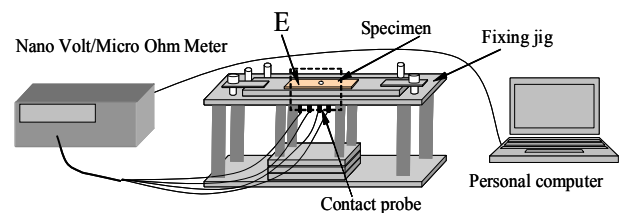
## 2.3. Electric resistance measurement

The electric resistance was measured using Micro Ohm meter (HP 34420A) under unloading at room temperature of 297 K in a process of fatigue testing, where a direct current potential drop technique was applied as shown in Fig. 3(a). Contact probe distance of A, B, C, D was 5 mm each to be shown in Fig. 3(b), and the stroke of a probe is 3 mm for contact between the probe and specimen. In this method, the direct current $I_{AD}$ passes through the outer pair of probes A and D, and $V_{BC}$ is the voltage between inner probes B and C. In addition, the measured value was inputted to a computer for every 3 seconds during measurement for 180 seconds. This was repeated five times and furthermore exchanged electricity direction five times. Finally, the mean value of all the measurement data is used as the electric resistance.

## 2.4. Residual stress measurement

The initial residual stress on the copper film before drilling a circular hole at the center of the specimen was measured using an X-ray stress measurement with Co-K$_\alpha$ line, the radiation area of 4.0×4.0 mm$^2$ and the X-ray stress constant of K=−112.0 MPa/deg. In addition, the incident angle was oscillated in a range of ± 2.5 deg, and the position of diffraction peak was determined by a half-value width method.

## 2.5. Ultrasonic testing measurement

Using an ultrasonic flaw detector image system (Honda Electronics HA701), a simple schematic diagram of the ultrasonic testing system is shown in Fig. 4(a), where a normally incident longitudinal wave with nominal frequency of 50 MHz was used for measuring the internal crack length.



(a) System of measuring electric resistance.
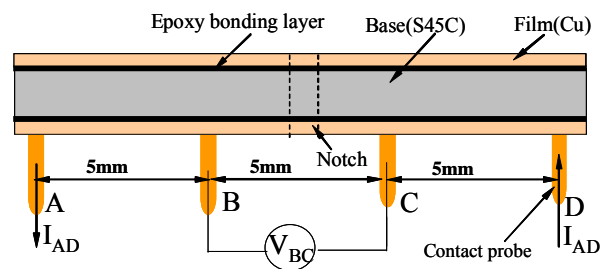


(b) Magnification of contact part (E).

Fig. 3. Schematic figure of measuring electric resistance.

(a) Ultrasonic testing system.
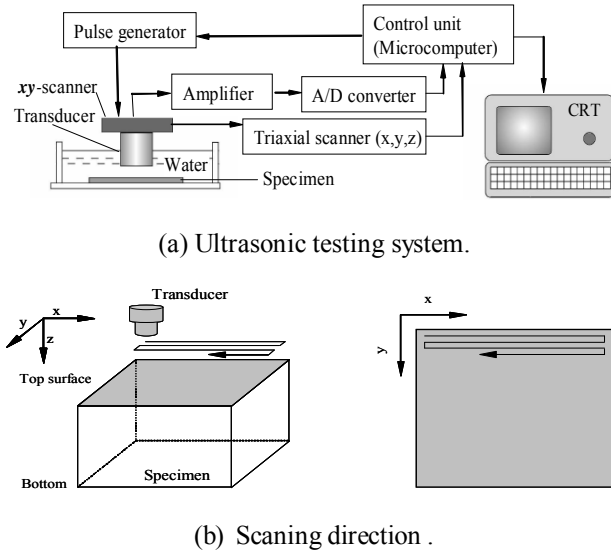


(b) Scaning direction .

Fig. 4. Schematic diagram of ultrasonic testing.

In order to achieve better reproducibility as well as fast and precise measurements, linear scanning was performed automatically using an x-y scanner. The space between transducer and the top surface of the specimen was filled with water under a constant temperature of 294 K as a medium for ultrasonic longitudinal wave propagation, and the distance between them was kept at 4.81 mm for focus of incident beam. A single flat pulse-echo transducer with radius of 1 mm was used for both generating and detecting the waves. All the received signals were amplified and then sent to a control unit, from which the digitized data were saved directly in a personal computer. For the scanning area, the transducer was automatically moved on the top surface along x and y axes in a scope area of $7.68 \times 7.68$ mm$^2$ with 0.02 mm steps, as shown in Fig. 4(b).

## 3. EXPERIMENTAL RESULTS

### 3.1. Residual stress and electric resistance on the film

As shown in Fig. 5, the initial residual stress was tension, because the linear thermal expansion coefficient is larger in the copper than the steel in Table 2. Namely, the residual stress is considered to be induced by the difference in the thermal shrinkage deformation mainly between the copper film and the base during the cooling process.

As shown in Fig. 6, the electric resistance, $R$, along width direction of specimen (x-axis) was measured in the copper film and the base specimen without a circular hole of notch. These measured values were compared with the theoretical values obtained from Eq. (1). In this equation, $F$ is the geometrical correction factor derived by Yamashita et al.[6], $t$ the sheet thickness and $\rho_v$ the resistivity where S45C has $\rho_v = 17.1 \times 10^{-8} \Omega$ m[7] and pure copper has $\rho_v = 1.724 \times 10^{-8} \Omega$ m[8].

$$R = \frac{V_{BC}}{I_{AD}} = \frac{\rho_v}{F \cdot t} \tag{1}$$

There is a remarkable agreement between the experimental and theoretical values for both copper film and base specimen. From this, it is found that this method is useful in measurement of the electric resistance in the copper film
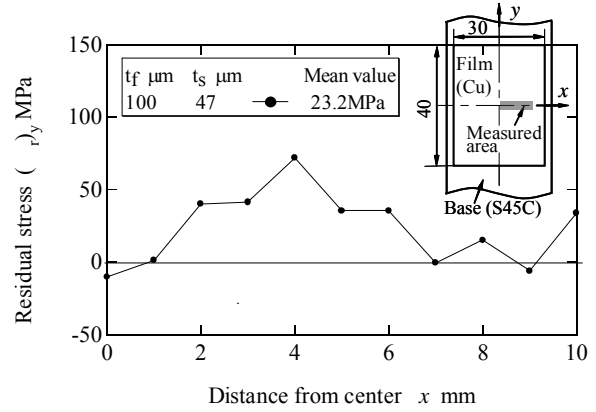


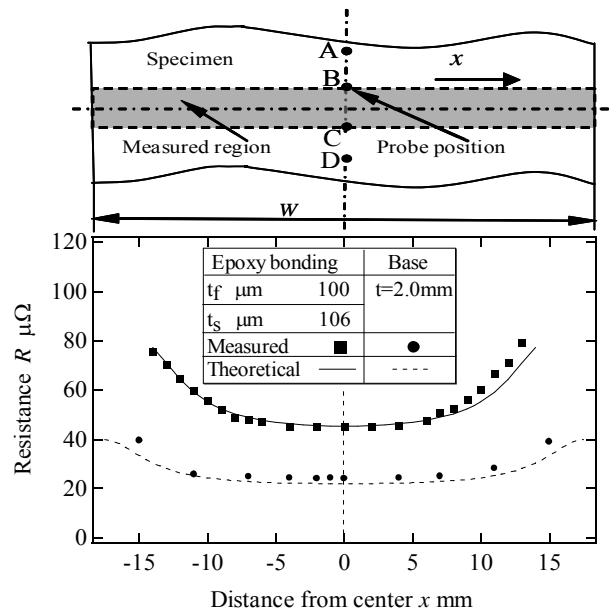Fig. 5. Residual stress distribution on the copper film.



Fig. 6. Electric resistance distributions on the surface.

even bonded to base with the resin layer. This means that the resin layer can be treated as the atmospheric air in the electric resistance measurement.

### 3.2. Fatigue crack propagation and electric resistance change

For the fatigue crack propagation curves shown in Fig. 7, using a half-length of crack, $a$ (including a circular hole of notch), plotted against the stress cycles, $N$, there is a difference between the bonded copper film and the base specimen. In this figure, side A and B show the front and back surfaces of the specimen respectively. The fatigue crack of the copper film propagated rapidly at the initial stage, but subsequently propagated slowly, and propagated rapidly again at the final stage. On the other hand, the fatigue crack of the base specimen propagated slowly at the initial and the subsequent stage, but propagated rapidly at the final stage. As a result, the fatigue crack propagation life is longer in the bonded copper film specimen than the base specimen.

The fatigue cracks were observed by scanning electron microscope (SEM) on the surface of epoxy-bonded copper film and the base specimen, as shown in Fig. 8 (a) and (b),
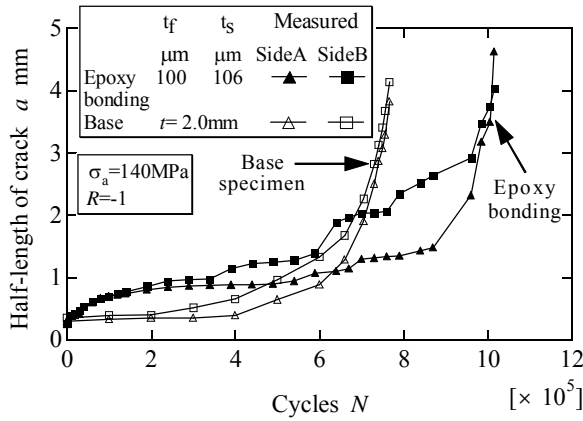
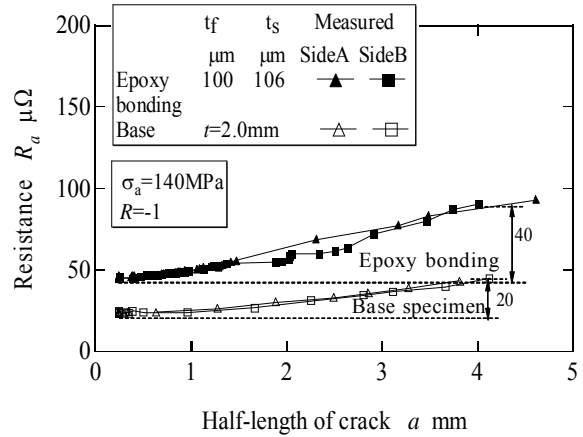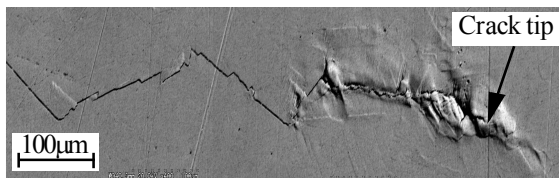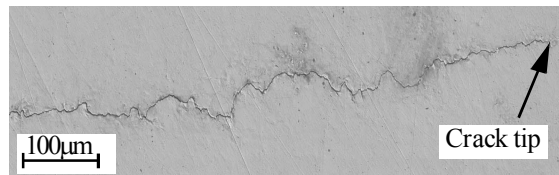Fig. 7. Fatigue crack propagation curves.



(a) Copper film bonded with resin ($t_f$=100μm, $N$=1.1×10⁶, $a$=4.70mm).



(b) Base specimen ($t$=2.0mm, $N$=1.42×10⁶, $a$=3.76mm).

Fig. 8. SEM micrographs of fatigue crack near the crack tip.

respectively. It can be seen that fatigue crack tip of copper film is opened on surface with tensile residual stress, as compared with that of the base specimen having the well-known crack closure.

The relationship between the electric resistance measured at the center of crack and the half-length of the propagated crack is shown in Fig. 9, where the electric resistance increases with the fatigue crack length. This result shows that the increase of electric resistance is due to the decrease of conductive area under crack propagaton. It should be noticed that the electric resistance much more increases in the copper film than the base specimen under the same crack length.
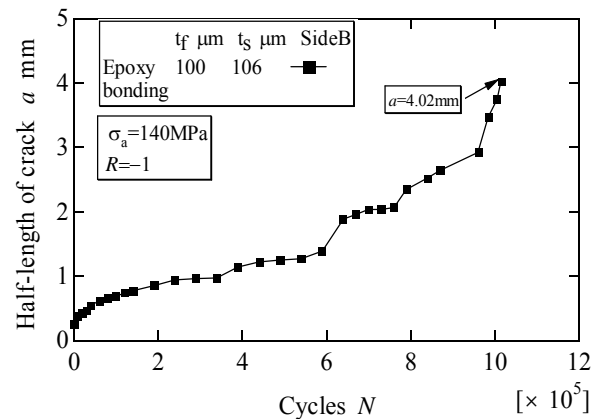
### 3.3. Crack detected by ultrasonic testing

The experimental ultrasonic velocity evaluated from the time through the thickness are in good agreement with the theoretical value calculated by Eq. (2) derived from a wave equation of isotropic elastic body[9], as shown in Table 3.

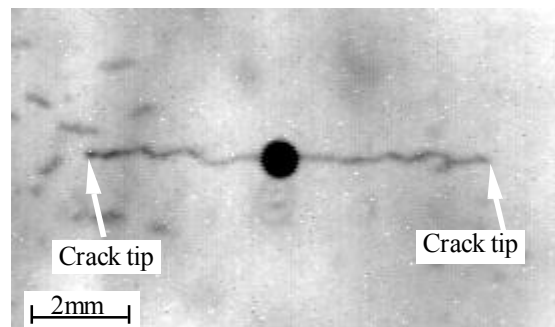$$c_l = \sqrt{\frac{\lambda + 2\mu}{\rho}} \qquad (2)$$

where $\lambda = \dfrac{\nu E}{(1+\nu)(1-2\nu)}$ , and $2\mu = \dfrac{E}{1+\nu}$



Fig. 9. Change of resistance due to crack propagation.

Table 3. Experimental and theoretical ultrasonic velocities.

|        | Experimental $c_l$ m/s | Theoretical $c_l$ m/s |
|--------|------------------------|------------------------|
| Cu     | 4755.2                 | 4604.4                 |
| Epoxy  | 2704.3                 | 2604.7                 |
| S45C   | 5998.5                 | 5962.6                 |



(a) Fatigue crack propagation curves of surface film.



(b) An example of internal crack observed by ultrasonic testing ($a$=4.02 mm, $d$=0.14 mm of A in Fig.11).

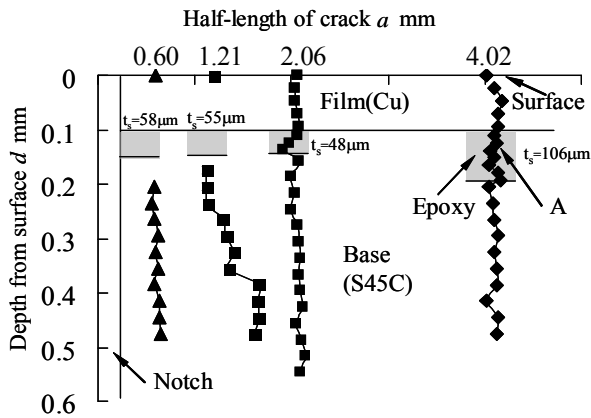Fig. 10. Crack propagation in the surface and inner part.

Fig. 11. Internal crack length measured by ultrasonic testing with the various surface crack length.

In this equation, $c_l$ and $\rho$ are sound wave velocity of longitudianl wave and density, respectively. In addition, Lame constants $\lambda$, $\mu$ are related with Young's modulus E and Poisson's ratio $\nu$ of Table 2. Using the experimental values of propagation veolocity, the distance from the specimen surface to internal crack was calculated using the measured wave propagation time.

The photograph of the internal crack detected by the ultrasonic testing, corresponding to the surface crack with the length of $a$=4.02 mm shown in Fig. 10(a), is shown as an example in Fig. 10(b). Using such photographs, the measured internal crack length along the depth, $d$, is shown in Fig. 11, corresponding to the surface crack length of $a$=0.60, 1.21, 2.06 and 4.02 mm measured by optical microscope for each specimen. From this, the internal fatigue crack is as long as fatigue crack of 0.6 mm on the surface, but subsequently the internal fatigue crack is longer than the surface crack length of 1.21 mm. Finally, the fatigue crack propagated uniformly through the thickness again from $a$=2.06 mm on the surface. This stage shows that the fatigue crack propagation on the surface was rapid as well as in the inner base, although fatigue crack propagation decelerated through the bonded epoxy resin layer as shown in Fig. 7. In this way, the use of ultrasonic testing proved its worth as a nondestructive measurement of the relationship between the internal crack and the surface crack length during fatigue.

## 4. DISCUSSIONS

### 4.1. Electric resistance change due to crack propagation

It was confirmed that the crack tip of copper film was opened in comparison with that of the base specimen as shown in Fig. 8. On the other hand, for a central slit in a plate with finite width of $W$, using a half-length of slit, $a$, and voltage, $V_a$ ($=V_{BC}$), between two middle probes B and C across a slit that is completely opened as shown in Fig. 12, Eq. (3) are indicated by Johnson[10]. In this equation, $a_0$ and $a$ are the initial and the subsequent crack length

$$\frac{V_a}{V_{a_0}}\left(=\frac{R_a}{R_{a_0}}\right)=\frac{\cosh^{-1}\left(\dfrac{\cosh \pi y/W}{\cos \pi a/W}\right)}{\cosh^{-1}\left(\dfrac{\cosh \pi y/W}{\cos \pi a_0/W}\right)} \qquad (3)$$
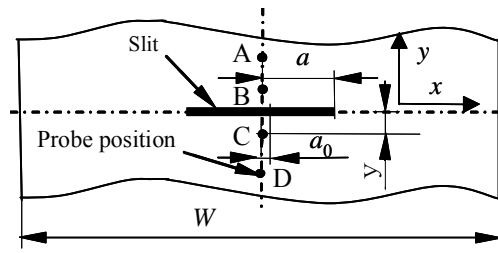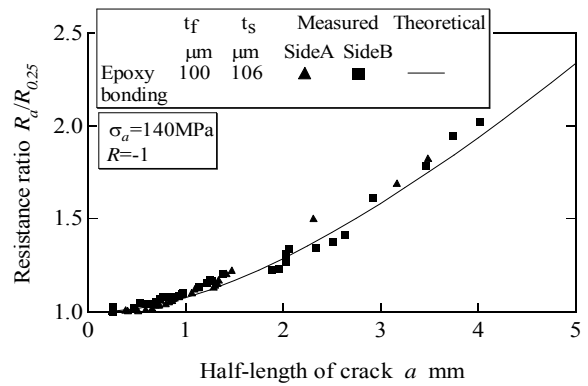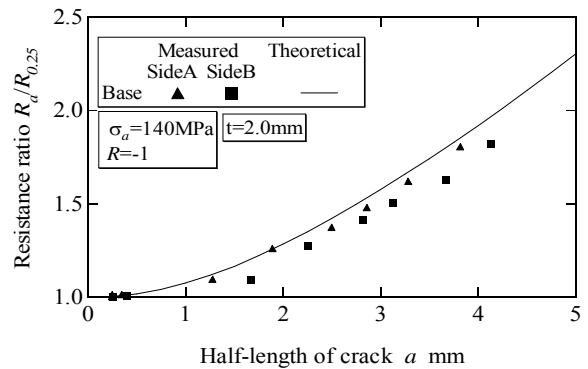


Fig. 12. Schematic figure of a central slit in a plate.



(a) Copper film bonded with resin.



(b) Base specimen.

Fig. 13. Measured and theoretical values of electric resistance ratio for various crack lengths.

respectively, and y is the half-distance between electrodes shown as probes B and C. In addition, the voltage $V$ and the resistance $R$ are shown with the suffix corresponding to $a_0$ and $a$, where $V_a/V_{a0}$ is equal to resistance ratio $R_a/R_{a0}$ under the same direct current. In the measured value of resistance ratio $R_a/R_{0.25}$ of copper film, the resistance of $R_{0.25}$ for the value of central hole radius with $a_0$=0.25 mm was used as the initial value in Eq. (3). As a result, there is a close agreement between the measured and theoretical values for the copper film in Fig. 13(a). In this way, the fatigue crack on copper film surface could be treated as a slit, because the crack was opened by the tensile residual stress. On the other hand, the measured values of the base specimen are slightly lower than the theoretical values in Fig. 13(b). From this, it is estimated that fatigue crack of the base specimen tends to produce partly contact in unloading with the plastic layer remained near the crack.

From the fact that the measured $R_a/R_{0.25}$ of the bonded copper film was in good agreement with the calculated value
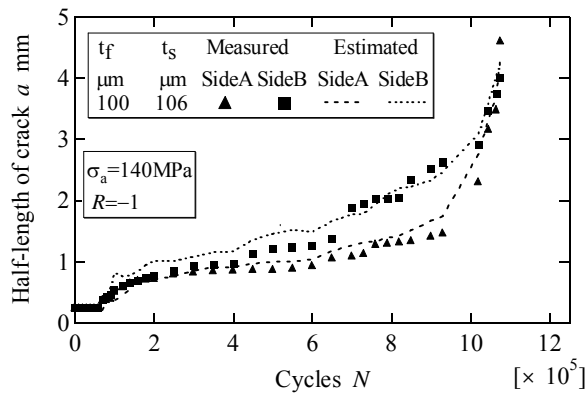
Fig .14. Measured and estimated fatigue crack
propagation curves.

by Fig. 13(a), it is found that the fatigue crack propagation curve can be estimated using Eq. (3) from the electric resistance measurement, as shown in Fig. 14.

### 4.2. Surface and internal fatigue crack propagation

According to the result obtained from the ultrasonic testing, there is no significant difference in the crack length between the inner base and the surface copper film at the initial stage with the surface crack length of $a$=0.60mm. At the subsequent stage, however, the internal crack of base is longer than the surface crack length of $a$=1.21mm on copper film. This is probably connected with the acceleration of fatigue crack propagation under plane strain condition near the central part of the inner base[11]. At the final stage over the surface crack length of $a$=2.06mm, the fatigue crack reached the same length in the base and film. From this, it is found that the effect of the insulation resin layer on the fatigue crack propagation of base and film gradually disappears with the increase of crack length in inner base of specimen.

### 5. CONCLUSIONS

The following conclusions were obtained on the basis of the experimental results using the electric resistance measurement and the ultrasonic testing for the copper film bonded with resin and the base specimen.
(1) Using specimen without a circular hole of notch , the distribution of the electric resistance measured by the direct current potential drop technique was in good agreement with the value calculated from the equation proposed for a finite plate. And then this method was used to measure the electric resistance of the specimens during fatigue crack

propagation.
(2) During fatigue crack propagation using the copper film bonded with resin, the electric resistance increased with the increase of crack length, these electric resistance changes were in good agreement with theoretical values reported for a slit in a finite plate, irrespective of crack length in inner base. This was because the fatigue crack of the surface copper film with tensile residual stress was opened even under unloading condition.
(3) As for the surface and internal cracks detected by ultrasonic testing, fatigue crack on the surface copper film and inner base propagated uniformly at the initial stage with the surface crack length of $a$=0.60mm, but subsequently propagated rapidly in the inner base. Finally, the fatigue crack of the surface copper film propagated rapidly again and reached to the same length as the inner base.

### REFERENCES

[1]  X. Fan, The Ninth Intersociety Conference on Thermal and Thermomechanical Phenomena in Electronic Systems, 2004. ITHERM '04., 2 (2004), 377-381.
[2]  A. J. Scholand, R. E. Fulton and B. Bras, Trans. ASME, J. Electron. Packag., 121(1999), 31-36.
[3]  Q.Yu and M. Shiratori, IEEE Trans. Comp., Packag. Manufact. Technol. A, 20(1997), 266-273.
[4]  Ron  S. Li, Trans. ASME, J. Electron. Packag., 123(2001), 394-400.
[5] A. Matsuba, T. Torii and D. H. Ma, Proceedings of InterPACK' 05, CD-ROM, IPACK2005-73168 (2005).
[6]  M. Yamashita and M. Agu, Jpn. J. Appl. Phys, 23(1984), 1499-1504.
[7]  Jpn Inst Metal, Metals handbook, Maruzen Publishers (1960),  28 (in Japanse).
[8]  Jpn Inst Metal, Metals data book, Maruzen Publishers (1974), 105 (in Japanse).
[9]   K. Nakamura, Ultrasonics, Corona Publishers(2001), p. 13 (in  Japanse).
[10] H. H. Johnson, Materials Research & Standards, l5(1965), 442-445.
[11] Y. Kondo and T. Endo, Current Reasearch on Fatigue Cracks, J. Soc. Mat. Sci., Japan,  (1985), 255 .